Metabolomics
DOI 10.1007/s11306-014-0667-5

ORIGINAL ARTICLE

Metabolomic profiling of bronchoalveolar lavage fluids by isotope labeling liquid chromatography mass spectrometry: a promising approach to studying experimental asthma

Jun Peng · Chris D. St. Laurent · A. Dean Befus · Ruokun Zhou · Liang Li

Received: 28 January 2014 / Accepted: 13 April 2014

Abstract Metabolomic analysis of bronchoalveolar lavage fluid (BALF) may help understand the pathophysiology of pulmonary diseases such as asthma. However, a major analytical challenge is that most metabolites in BALF are in low abundance and further diluted by the collection procedure. Here we report a sensitive metabolomic profiling method based on ^{12}C-/^{13}C-differential isotope dansylation that targets amine- and phenol-containing metabolites, solid phase extraction for analyte enrichment, and liquid chromatography Fourier transform ion cyclotron resonance-mass spectrometry (LC–FTICR-MS). This method detected 250 ion pairs or putative metabolites in rat BALF and 36 of them were positively identified. The majority were not reported in previous studies using NMR or conventional LC–MS. The developed isotope labeling method was then applied to investigate metabolomic changes in BALF samples from a model of allergic asthma in rats. Statistical analysis of the resultant data showed that there was distinct separation between normal and inflamed rats. Metabolic pathway analysis indicated that the arginine-proline metabolic pathway was dysregulated in rats with experimental asthma.

Keywords Allergic asthma · Airways inflammation · Animal models · Bronchoalveolar lavage fluid · Metabolomics · LC–MS

1 Introduction

Asthma is a global health problem that in 2010 affected 300 million people (Locksley 2010). It is a heterogeneous syndrome with many clinical classifications. Allergic asthma is the most common form, and allergic inflammation is an important pathophysiological feature, involving several cell types including: epithelial cells, smooth muscle cells, mast cells, dendritic cells, eosinophils, neutrophils, macrophages and T and B lymphocytes (Galli et al. 2008). However, the pathogenesis is incompletely understood and there is no objective diagnostic biomarker of asthma in a typical clinical setting (Adamko et al. 2012).

Bronchoalveolar lavage (BALF) is a procedure for sampling the lumen of the respiratory tract using a bronchoscope (Connett 2000; Reynolds 2000) and a saline wash (Meyer 2004). BALF contains different cell types and a variety of soluble substances, such as protein and small molecule metabolites (Walters et al. 1996). Chemical analysis of BALF may aid in diagnosis and in definition of pathophysiological mechanisms of pulmonary disease, as BALF is in close proximity to lung tissue, and thus likely to be a better source of biomarker discovery than other biofluids, such as urine and blood. Analysis of cells in BALF can be useful in diagnosis of some pulmonary diseases; however, it lacks sensitivity and specificity (Szefler et al. 2012). Accordingly, there is interest and clinical need for development of novel assays of BALF for pulmonary diseases.

Electronic supplementary material The online version of this article (doi:10.1007/s11306-014-0667-5) contains supplementary material, which is available to authorized users.

J. Peng · R. Zhou · L. Li (✉)
Department of Chemistry, University of Alberta, Edmonton, AB, Canada
e-mail: Liang.Li@ualberta.ca

C. D. St. Laurent · A. D. Befus (✉)
Department of Medicine, University of Alberta, Edmonton, AB, Canada
e-mail: dean.befus@ualberta.ca

Published online: 11 May 2014

Metabolomics seeks to study the complete set of small molecule metabolites in a biological sample using a holistic and unbiased approach. The metabolome measurement can provide a functional readout of the physiological and pathophysiological state and has potential to identify novel biomarkers and help to understand molecular mechanisms of disease (Atzei et al. 2011; Kominsky et al. 2010). Metabolomic profiling of urine and breath samples has been used to investigate asthma (Saude et al. 2009, 2011; Carraro et al. 2007), but until recently metabolomic profiling of BALF has not been widely used. The metabolite level in BALF can be relatively low compared with blood or urine and presents an analytical challenge (Serkova et al. 2008; Walters et al. 1996). A few metabolomics studies of BALF have been reported in humans (Wolak et al. 2009), mice (Hu et al. 2008), and rats (Azmi et al. 2005) and most studies used NMR spectroscopy, a relatively insensitive method with limited metabolome coverage. Gas chromatography MS (GC–MS) was applied to analyze BALF from human infants (Fabiano et al. 2012) and more recently, GC–MS along with LC–MS was used to analyze BALF in allergic airways inflammation in mice and revealed novel changes in lung metabolic pathways as compared with normal controls (Ho et al. 2013). However, using both positive and negative ion modes of conventional LC–MS, this work only detected about 300 features in BALF, compared to thousands of features in urine or serum/plasma samples. Moreover, <20 % of detected features are actually from unique metabolites in LC–MS analysis of biofluids (Jankevics et al. 2012). Clearly, there is a need to develop a more sensitive LC–MS technique for metabolome profiling of BALF samples with greater metabolome coverage.

We recently developed a differential ^{12}C-/^{13}C-dansylation isotope labeling LC–FTICR-MS method for profiling metabolites containing primary, secondary amine or phenol groups (Guo and Li 2009). This method can enhance sensitivity by 1–3 orders of magnitude and improve quantification precision using ^{13}C isotopic global internal standards. It has been used in metabolic profiling of a variety of biological samples to discover potential metabolite biomarkers and cellular metabolomics (Zheng et al. 2012; Wu and Li 2013). Here we report a method based on dansyl-labeling LC–MS for metabolomic profiling of rat BALF samples and apply this to investigate experimental allergic asthma in rats.

2 Materials and methods

2.1 Chemicals and reagents

All the chemicals and reagents, unless otherwise stated, were purchased from Sigma-Aldrich Canada (Markham, ON, Canada). For dansylation labeling reactions, the ^{12}C-labeling reagents were from Sigma-Aldrich and the ^{13}C-labeling reagents were synthesized in our lab using the procedures published previously (Guo and Li 2009). LC–MS grade water, methanol, and acetonitrile (ACN) were purchased from ThermoFisher Scientific (Nepean, ON, Canada).

2.2 Rat model and sample collection

We used a widely studied rat model of allergic asthma known to induce IgE and IgG antibodies and both neutrophilia and eosinophilia (Elwood et al. 1991; Waserman et al. 1992; Haczku et al. 1994). Male 10-week old Brown Norway rats (Harlan Sprague-Dawley, Indianapolis, IN) were housed in the Health Sciences Laboratory Animal Services (University of Alberta, Edmonton, Alberta, Canada), on a 12-h light–dark cycle, with access to food and water ad libitum. The animals were rested for a minimum of 1 week after arrival before experimentation. Rats were sensitized to ovalbumin (OA) with an intraperitoneal injection of 10 μg OA, 50 ng pertussis toxin, and 150 mg aluminum hydroxide (a protocol optimized for sensitization and IgE production) (Dery et al. 2004). On d 21 rats were challenged for 5 min with a 5 % OA solution or saline using a Micro Mist nebulizer (Hudson RCI, Durham, NC). This work was approved by the University of Alberta Health Sciences Animal Policy and Welfare Committee in accordance with guidelines of the Canadian Council on Animal Care.

To minimize day-to-day variation, all animal experiments were conducted by a single investigator using standardized methods. 24 h following OA challenge, rats were euthanized, the trachea was cannulated with polyethylene tubing and 5 mL of ice-cold phosphate buffered saline (PBS) was instilled into the airways and the lungs were gently massaged. The PBS was aspirated into ice-cold polypropylene tubes and the 5 mL instillation and removal was repeated six times. For the first 5 mL instillation, 2–2.5 mL was recovered, kept separate and following cell collection by centrifugation (see below), the fluid was stored in a −80 °C freezer to be used for metabolomic analysis. The remaining BALF collected (on average 23 mL of 25 mL instilled) was centrifuged for 5 min at 300×g to pellet the cells, combined with cell pellets from the initial 2 mL, resuspended in PBS, and cell viability (>95 %) determined by trypan blue exclusion. The cells were counted and cell smears were prepared using a Cytospin (Thermo Fisher Scientific). Cell differentials (minimum of 300 cells assessed) were determined following staining with PROTOCOL Hema 3 staining system (Thermo Fisher Scientific).

2.3 BALF sample preparation

Figure 1 shows the workflow for sample preparation and LC–MS analysis. A pooled sample was generated from aliquots of 36 rat BALF samples (from the 36 rats listed above, both control and inflamed rats). 50 µL of each of 36 rat samples was ^{12}C-dansylation labeled (see next section). 50 µL of the pooled sample was ^{13}C-dansylation labeled. After they were combined, the mixture was run through solid phase extraction (SPE Oasis HLB cartridge, Waters Limited, Mississauga, Ontario, Canada). The SPE cartridge was first conditioned with methanol, then equilibrated with water and after the sample was loaded, the cartridge was washed with water to remove the salts. The sample was eluted with ACN and the eluate was concentrated 10.5 times using a SpeedVac and was injected into LC–MS.

A 50 µL aliquot of the pooled sample that was ^{12}C-dansylation labeled was mixed with a 50 µL aliquot of the pooled sample that was ^{13}C-dansylation labeled. This mixture was used as a quality control (QC) sample. It was run through SPE, followed by analyte enrichment, just as in the case of a sample mixture. There were four QC samples prepared in this way. Each QC sample was injected twice. Thus, there were a total of 8 QC injections. Each QC injection was followed by 5 sample injections except the last batch with 6 sample injections for a total of 36 samples.

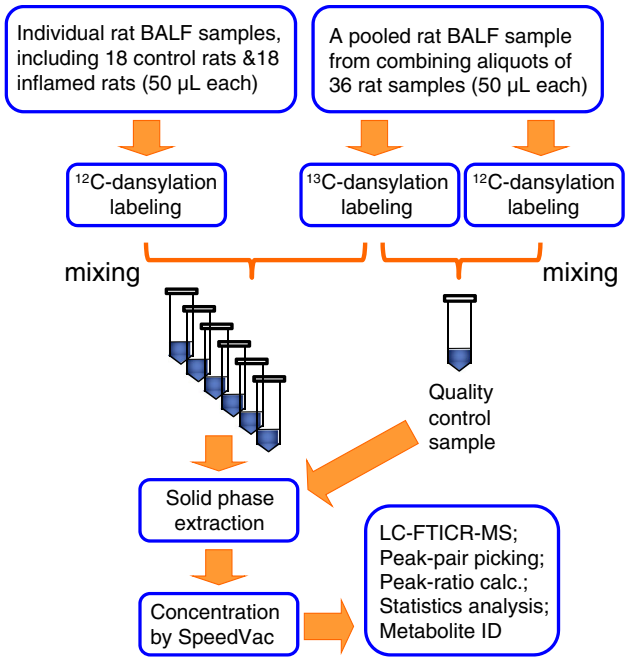

Fig. 1 Experimental workflow of isotope labeling LC–MS for comparative metabolomics between 18 control rats (naive [n = 9] pooled with sensitized but saline challenged, n = 9) and 18 sensitized rats challenged with aerosolized ovalbumin (inflamed). The pooled BALF sample was generated from aliquots of 36 rat BALF samples and used as a global internal standard

2.4 Dansylation labeling

All the dansylation labeling reactions for rat BALF samples were adapted from our previous report (Guo and Li 2009). Briefly, 50 µL of the sample was mixed with 50 µL sodium carbonate/sodium bicarbonate buffer (0.5 mol/L, pH 9.5) in reaction vials. 50 µL of freshly prepared ^{12}C dansyl chloride solution (20 mg/mL) was added to each of individual sample for light labeling. 50 µL of ^{13}C-dansyl chloride solution (20 mg/mL) was then added to each pooled sample for heavy labeling. The dansylation reaction was performed in an Innova-4000 bench top incubator shaker (New Brunswick Scientific, Enfield, CT, USA) at 60 °C for 60 min. Finally, 10 µL of a 250 mM sodium hydroxide solution was added to quench the reaction.

2.5 Sample preparation for method development

Pooled normal rat BALF was split into two identical aliquots of 100 µL. One aliquot was ^{12}C-dansylation labeled and the other aliquot was ^{13}C-dansylation labeled. They were combined into one vial. After adjusting pH to 3, the mixture was run through SPE. For the absolute quantification, one aliquot of pooled normal rat BALF sample was ^{12}C-dansylation labeled and then spiked with a fixed amount of authentic standard which was ^{13}C-dansylation labeled. Calibration was prepared by using a series of concentrations of a mixture of authentic standards, which were ^{12}C-dansylation labeled. They were spiked into the fixed amount of authentic standard, which was ^{13}C-dansylation labeled.

2.6 LC–MS

An Agilent 1100 series binary system (Agilent, Palo Alto, CA) and an Agilent reversed-phase Eclipse plus C18 column (2.1 mm × 100 mm, 1.8 µm particle size, 95 A pore size) were used for LC–MS. LC solvent A was 0.1 % (v/v) LC–MS grade formic acid in 5 % (v/v) LC–MS grade ACN, and solvent B was 0.1 % (v/v) LC–MS grade formic acid in LC–MS grade ACN. The gradient elution profile was as follows: t = 0 min, 20 % B; t = 3.0 min, 35 % B; t = 16 min, 65 % B; t = 18.6 min, 95 % B; t = 21 min, 95 % B; t = 21.3 min, 98 % B; t = 23.0 min, 98 % B; t = 24.0 min, 20 % B. The flow rate was 150 µL/min. The flow from RPLC was split 1:2 and a 50 µL/min flow was loaded to the electrospray ionization (ESI) source of a Bruker 9.4 Tesla Apex-Qe Fourier transform ion-cyclotron resonance (FTICR) mass spectrometer (Bruker, Billerica, MA, USA), while the rest of the flow was delivered to waste. All MS spectra were obtained in the positive ion mode.

The same LC equipment with the same LC running conditions was connected with QTRAP 2000 quadrupole

linear trap mass spectrometer (AB Sciex, Concord, ON, Canada) to do the absolute quantification work.

2.7 Data analysis

An integrated approach was used to do the automated data preprocessing. The XCMS software (Smith et al. 2006) was used for peak picking from the LC–MS data. An in-house written R program was used to find ^{12}C-/^{13}C-dansyl labeled peak pairs based on the mass difference of 2.00671 Da of isotopic pairs and the mass accuracy tolerance of 2 ppm. The relative ion intensity of ^{12}C-labeled/^{13}C-labeled pairs was calculated. The redundant peaks of each metabolite, such as natural isotopic peaks, sodium/potassium/ammonia adduct peaks, doubly or triply charged peaks, and dimer peaks, were automatically removed by the program.

Multivariate statistical analysis was carried out using SIMCA-P+ 11.5 (Umetrics AB, Umea, Sweden). PCA, partial least squares discriminant analysis (PLS-DA) and orthogonal projections to latent structures discriminant analysis (OPLS-DA) were used to analyze the data. One hundred permutation tests, built in SIMCA-P, were used to conduct cross validation for the OPLS-DA model. A list of top important metabolites which contributed most to the model was generated from the variable importance of the projection (VIP) plot. There were 48 metabolites with VIP score of greater than 1.0. Among them, 44 metabolites were also found in the PLS-DA model (Supplemental Table T1). A web-based software Metaboanalyst (Xia et al. 2009) was used to construct the heat map using hierarchical clustering method, and to perform the *t* test, calculate the *P*-value and fold change for individual metabolites. Correlations between the important metabolites and inflammatory cells were calculated using Pearson's correlation analysis built in Metaboanalyst 2.0.

2.8 Metabolite identification

The potential metabolite biomarkers were selected based on their rank in VIP value in the OPLS-DA model, *P*-value, and fold changes. Each metabolite had its retention time and accurate mass information. Mass of the underivatized metabolites was obtained by subtracting the measured mass of the dansylation labeled metabolite from the dansyl group. The MycompoundID program (Li et al. 2013) was used to search the accurate mass within the human metabolome database (Wishart et al. 2009) with a mass accuracy tolerance of 5 ppm. The metabolite markers were definitively identified if they were matched with the retention time and accurate mass of authentic standards under the same experimental conditions. The matched metabolites were deemed to be putatively identified if their authentic standards were not available.

2.9 Metabolic pathway analysis

The construction and analysis of metabolic pathways of potential biomarkers was performed using a web-based tool, MetPA (Xia and Wishart 2010) that was associated with Metaboanalyst 2.0 software (http://metpa.metabolomics.ca/MetPA/). MetPA combines advanced pathway enrichment analysis along with analysis of pathway topological characteristics to identify and visualize the most relevant metabolic pathways.

3 Results and discussion

3.1 Method development

Dansylation labeling can improve the detection of amine- and phenol-containing metabolites (Guo and Li 2009). Initially we applied dansylation labeling to the rat BALF samples directly, followed by injection into LC–MS, as we would do for other biofluids, such as urine. However, few peaks were detected in the ion chromatogram (see Fig. 2a).

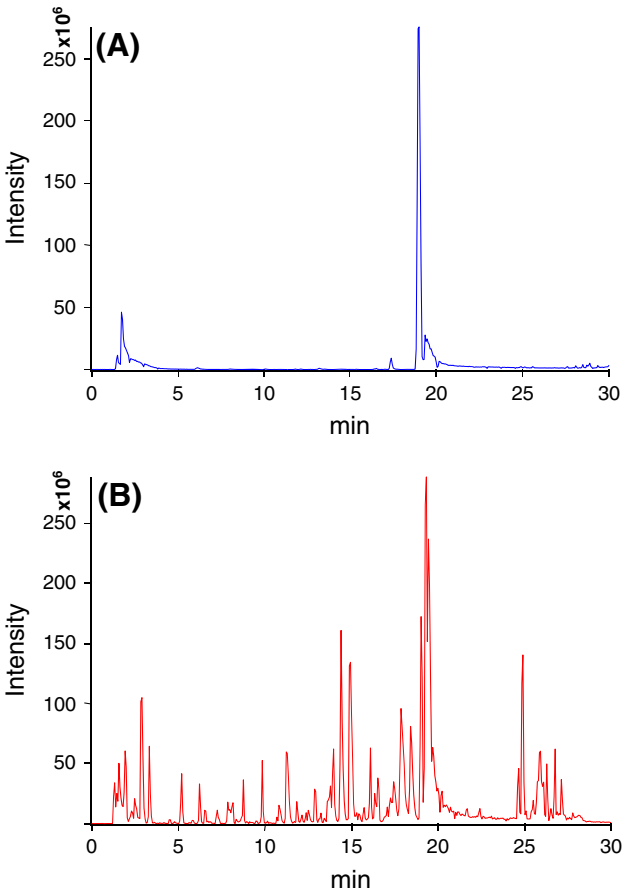

Fig. 2 Base-peak ion chromatograms obtained **a** without SPE and analyte concentration and **b** with SPE and analyte concentration

The earlier elution peaks were from the quenched labeling reagent, dansyl hydroxide, and the intense peak at around 19 min was from an unknown impurity with m/z 266.0833; the mass spectra of this peak only shows a single peak, not peak pair. Low metabolite detectability is due to low concentrations of metabolites in BALF collected using a washing procedure. Because of high concentrations of sodium phosphate buffer and salts, it was not feasible to use solvent evaporation to concentrate the metabolites. To overcome this challenge, we developed an analytical strategy using reversed phase SPE to remove high concentrations of buffer, salts and other impurities after dansylation labeling of the metabolites. The SPE eluate was concentrated before injecting into LC–MS. A 10.5 fold increase in analyte concentration was achieved while removing salt interference in LC–MS.

Figure 2b shows the ion chromatogram of normal rat BALF obtained using dansyl labeling, SPE and LC–MS. About 250 unique peak pairs were detected, most probably corresponding to 250 different metabolites containing primary, secondary amine or phenol groups. While applying SPE for analyte concentration is straightforward, the pH of the samples should be controlled to generate reproducible results. We studied the effect of different pH of the samples before loading into the SPE cartridge, and found that pH 3 was the best condition compared with pH 7 and pH 10 (Supplemental Figure S1). At pH 10, about 200 peak pairs were detected and 50 of them were different from the 250 peak pairs found at pH 3. While it is possible to expand the metabolite coverage by combining the results from different SPE fractions, sample consumption and analysis time would increase, and thus in this particular work only the pH 3 fraction was analyzed.

3.2 Metabolite identification and absolute concentrations

Among the 250 peak pairs detected, we identified 36 metabolites based on matching mass and retention time with their authentic standards; our current standard library contains 296 metabolites. Supplemental Table T2 shows the list of metabolites positively identified. The majority of them were not identified by previous NMR study of rat BALF samples (Azmi et al. 2005) and mouse BALF samples using LC–MS (Ho et al. 2013).

There are no reports on the absolute quantification of metabolites in rat BALF samples. To fill this knowledge gap, we developed a scheduled multiple reaction monitoring (MRM) method using QTRAP mass spectrometry to quantify some of the metabolites in normal rat BALF samples. Supplemental Figure S2 shows the ion chromatogram for quantification of 24 metabolites in rat BALF using the MRM method. These 24 metabolites were selected after considering the 36 metabolites identified in BALF and others arbitrarily chosen from our compound library. We validated the internal standard method by comparing the results obtained with the standard addition method for two metabolites, glycine and alanine. Supplemental Table T3 shows results obtained by the two methods; quantitative results were essentially the same. This is not surprising, as we used SPE in our LC–MS quantitative analysis that would minimize the matrix effect in analyte quantification. Supplemental Table T4 lists the information on the absolute concentrations of 24 metabolites in normal rat BALF. The concentrations of 15 metabolites range from 6.7 nM to 3.93 μM, whereas concentrations of the other 9 metabolites are below the limit of quantification (50 nM except 5 nM for cresol). These results indicate that metabolite concentrations in BALF are very low, presenting a major detection challenge to conventional metabolome profiling techniques such as NMR and LC–MS. However, dansyl labeling LC–MS can provide a means of detecting many amine- and phenol-containing metabolites in BALF. Note that, using the QTRAP2000 mass spectrometer which is not very sensitive, compared to the latest model, the 9 metabolites could not be detected using the MRM method. However, they were detectable in the full scan mode of the more sensitive FT-ICR-MS instrument.

3.3 Comparative metabolome analysis between inflamed rats and control rats

A total of 36 rats were used, including: 18 inflamed rats sensitized with OA and challenged with aerosolized OA, and 18 control rats comprised of 9 naïve rats and 9 rats sensitized with OA but challenged with saline, not OA. Cell counts and differential analysis established that naïve rats and rats sensitized with OA but challenged with saline had similar cell profiles in BALF. In these experiments, rats not sensitized to OA but challenged with saline were not studied, as earlier investigations by ourselves and others have shown that this protocol does not induce inflammatory responses in BALF (Schuster et al. 2000; Maghni et al. 2000).

We have developed a workflow (Fig. 1) that incorporated SPE in sample handling for differential isotope labeling of amine- and phenol-containing metabolites of BALF samples. During the data collection, a QC sample (see Fig. 1) was used to confirm if the analytical performance was robust. Figure 3a shows the PCA plot of the individual rat samples as well as the QC samples. All QC sample injections (8 injections in total from four QC samples) were tightly clustered (labeled as black dots in Fig. 3a). This indicates that overall technical variation was small. PCA is an unsupervised model, which can provide an overview of the dataset revealing general trends,

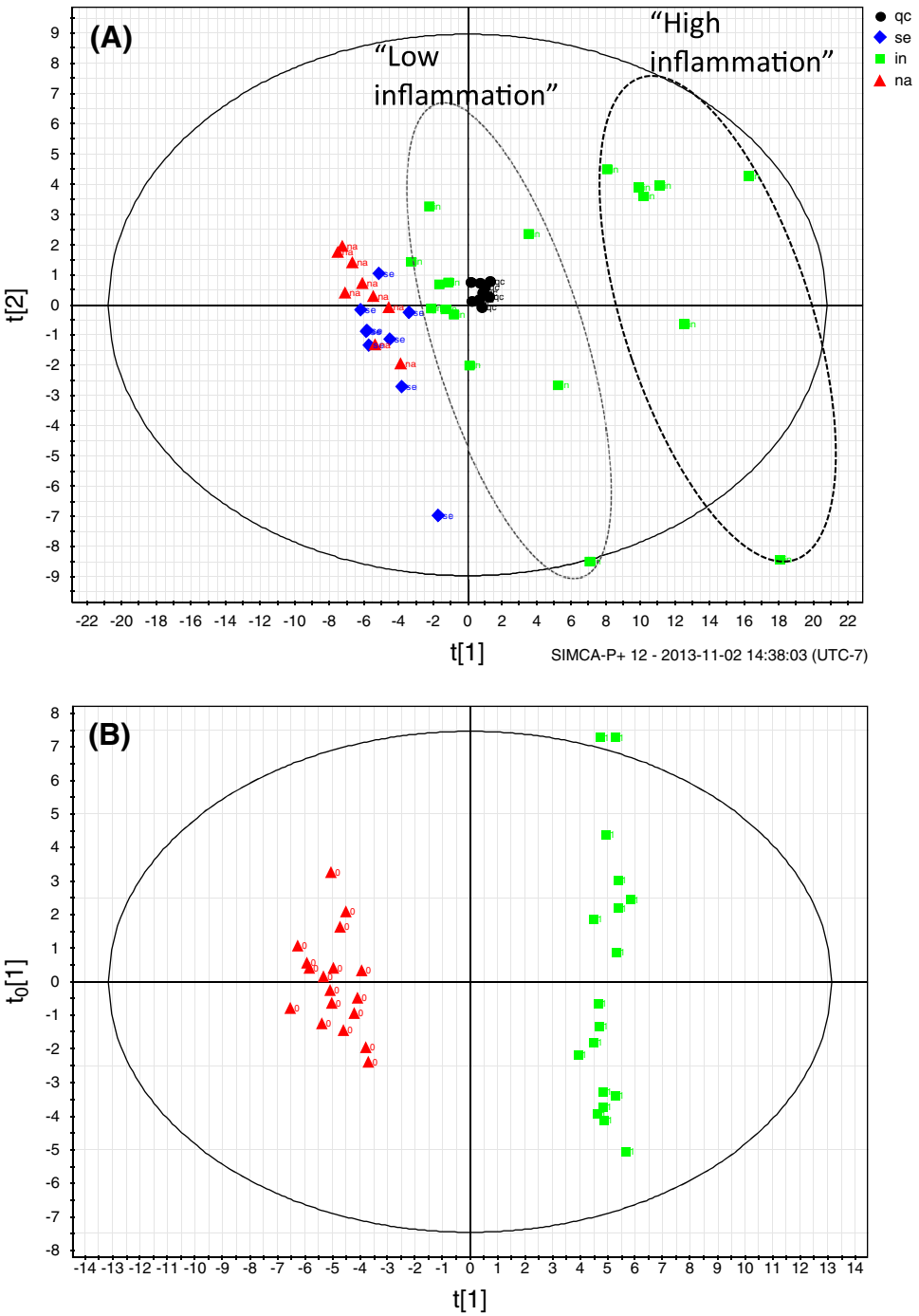

Fig. 3 **a** Score plot of PCA showing some separation between 9 naïve rats (*red triangles*), 9 rats sensitized but saline challenged (*blue diamonds*), and 18 inflamed rats (*green squares*); *black dots* were from 8 injections of the quality control sample. **b** Score plot of OPLS-DA showing distinct separation between 18 control rats (*red triangles*) and 18 inflamed rats (*green squares*) (Color figure online)

clustering and outliers. Figure 3a shows that there was no obvious separation between 9 naïve rats (labeled as red triangles) and 9 rats sensitized with OA, challenged with saline (labeled as blue diamonds). This data also established that the use of pertussis toxin and aluminum hydroxide as adjuvants for OA immunization did not significantly alter the base metabolome profile in BALF. In contrast, there is clear separation between 18 inflamed rats (all labeled as green squares) and 18 control rats. In this PCA model, R^2X (cum) = 0.49, Q^2 (cum) = 0.39.

OPLS-DA, a supervised model, was used to maximize the separation and enhance model visualization and interpretation. Figure 3b is the score plot of OPLS-DA showing that there was distinct separation between 18 control rats (red triangles) and 18 inflamed rats (green squares). In this OPLS-DA model, R^2X (cum) = 0.59, R^2Y (cum) = 0.98,

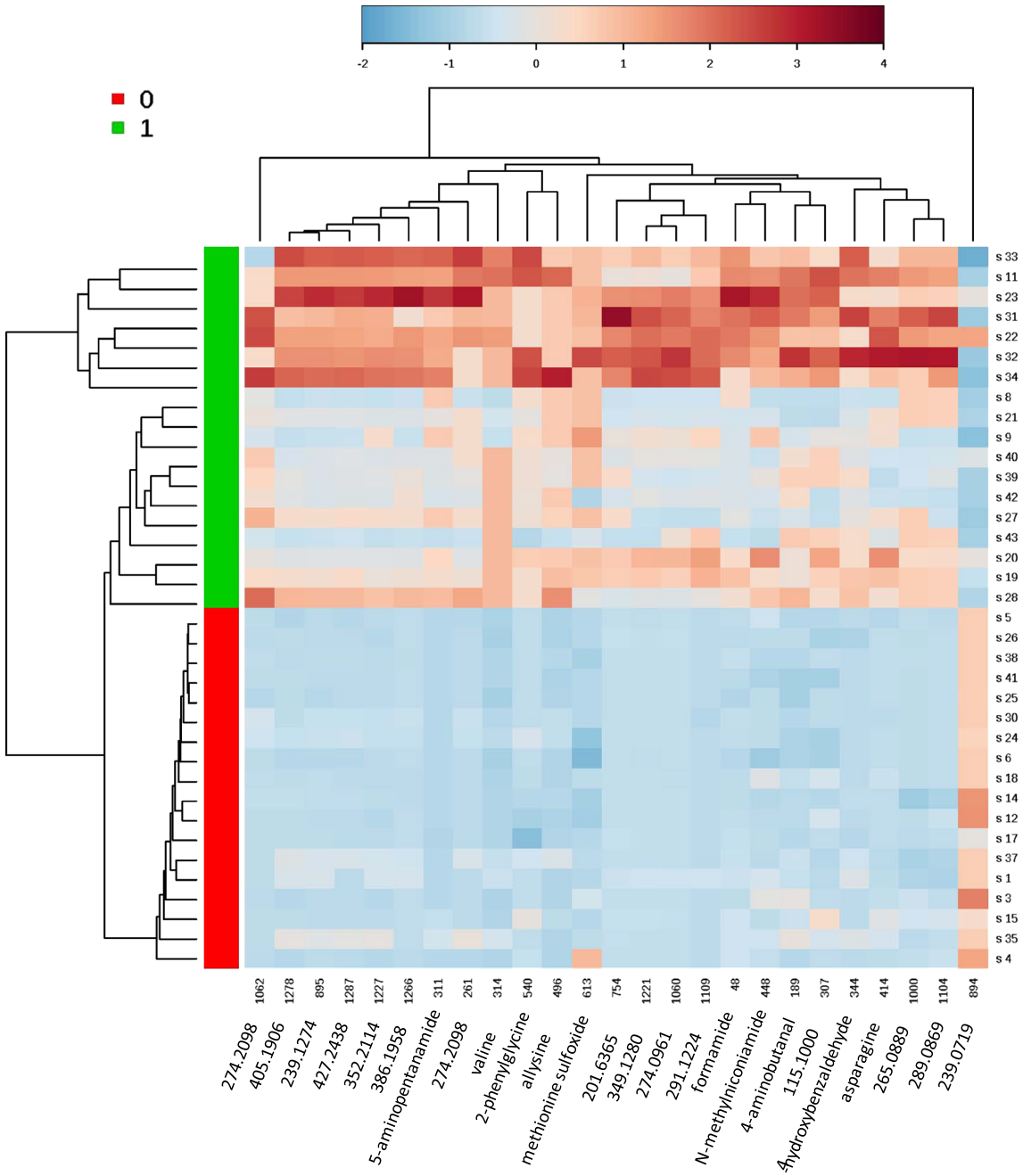

Fig. 4 Heat map generated by the hierarchical clustering method. The rows are individual rat samples and the columns are the top 25 important metabolites selected on the basis of their *P* values in a *t*-test. For those metabolites that are definitely or putatively identified, their name is given, and for those not identified, their accurate mass is provided on the x axis. All 18 control rats are clustered together at the *bottom half labeled with red* and all 18 inflamed rats are clustered together at the *top half labeled with green* (Color figure online)

Q^2 (cum) = 0.91. Since OPLS-DA is prone to overfitting, we did cross validation using the 100 permutation test. The validation plot shown in Supplemental Figure S3 indicates that the original model was valid, as the Q2 regression line has a negative intercept and all permutated R2 and Q2 values to the left are lower than the original point to the right.

HCA is another unsupervised chemometrics method. A dendrogram was generated to see the hierarchical structure of all samples and a heat map was constructed to visualize the intensities of individual metabolites. Figure 4 shows the heat map of metabolomic profiles between 18 control rats and 18 inflamed rats, using intensity information of the top 25 metabolites (selected based on their *P* value in the

Table 1 Metabolites dysregulated in a rat model of allergic airways inflammation

Metabolites	RT (min)	Mass dansylated	Mass underivatized	Mass accuracy (ppm)	*T* test (*P* value)	Fold change	VIP score	Remarks
Valine	11.93	351.13762	117.07929	2.30	1.50E−02	3.4	1.70	Definitive
4-Aminobutanal	13.22	321.12693	87.06861	2.20	1.68E−06	3.2	1.40	Putative
4-Hydroxybenzaldehyde	24.63	356.09566	122.03734	4.55	1.50E−03	4.4	1.35	Definitive
2-Phenylglycine	16.92	385.12207	151.06374	2.73	5.00E−03	3.3	1.34	Definitive
Formamide	11.43	279.07984	45.02151	1.06	1.90E−04	5.3	1.30	Putative
Asparagine	4.51	366.11206	132.05373	1.80	3.20E−04	4.1	1.29	Definitive
Proline	13.59	349.12183	115.06351	1.56	3.50E−05	2.7	1.23	Definitive
Hydroxyproline	7.49	365.11675	131.05842	1.35	6.80E−03	2.4	1.19	Definitive
Alanine	10.37	323.10616	89.04783	1.72	8.30E−05	2.6	1.19	Definitive
Threonine	8.14	353.11676	119.05843	1.56	1.40E−05	2.4	1.17	Definitive
Xanthine	11.99	386.09198	152.03365	1.50	1.60E−03	−3.9	1.11	Definitive
Arginine	3.61	408.17033	174.11200	1.86	4.00E−03	2.3	1.10	Definitive
Ammonia	8.22	251.08482	17.02650	3.00	1.80E−02	1.8	1.10	Definitive

t-test). All 18 control rats cluster at the bottom and all 18 inflamed rats cluster at the top of the heat map, consistent with the PCA and OPLS-DA results.

We also did the PCA and HCA analysis only using 9 naïve rats and 9 rats sensitized, challenged with saline (see Supplemental Figures S4 and S5). There is no clear metabolomic difference between the two subgroups.

3.4 Metabolite biomarkers and pathway analysis

Among the most significant metabolites, we definitively identified 11 metabolites based on matching retention time and accurate mass with their authentic standards under the same experimental conditions. We also putatively identified 2 metabolites based on accurate mass matches alone, which were not validated since their authentic standards were not commercially available. The list of the top important metabolites identified includes: arginine, proline, hydroxyproline, ammonia, 4-hydroxybenzaldehyde, asparagine, valine, alanine, threonine, 2-phenylglycine, xanthine, formamide, and 4-aminobutanal (Table 1). Most of these metabolites were up-regulated in inflamed rats and only one metabolite, xanthine was down-regulated in inflamed rats. *T*-tests for these 13 metabolites showed that their concentrations were significantly different between the groups. The fold changes of these metabolites are also distinct, ranging from 1.8 to 5.3.

Metabolic pathway analysis was used to determine if these metabolites are related to specific metabolic pathways. The web-based tool, MetPA, combines powerful pathway enrichment analysis with pathway topology analysis to help identify the most relevant pathways. Pathway topology particularly takes into account that centered positions of a network will have a bigger impact in that pathway than marginal or relatively isolated positions. Applying MetPA to our data indicates that it is highly probable that the arginine-proline pathway was dysregulated in allergic inflammation in the lung. Figure 5 shows the perturbed arginine-proline pathway, where five dysregulated metabolites including arginine, proline, hydroxyproline, ammonia, and 4-aminobutanal are highlighted in red.

3.5 Cell count analysis and its potential relevance to metabolomic profiling

Although the rats are inbred and we used rigorously standardized methods, there was variability among the inflamed rats in the PCA model and separation in two subgroups, we arbitrarily labeled low and high inflammation (Fig. 3a). The heat map (Fig. 4) also identified these two clusters in the inflamed rats; the top 7 samples in one subgroup and the bottom 11 samples in another subgroup. The separation of individual animals in the heat map fully aligned with the subgroup separation in PCA in the inflamed rats. We then tested if there was correlation between metabolomic profiles and inflammatory cell numbers in BALF samples, total cell counts and differential cell analysis including eosinophils, neutrophils, and macrophages (Table 2; Supplemental Tables T5 and 6).

Figure 6 shows comparisons among the total leucocyte numbers, neutrophils, eosinophils and macrophages in BALF from control rats and OA challenged, sensitized rats in the low and high inflammation subgroups. For all panels (a–d) the cell numbers in both the low and high

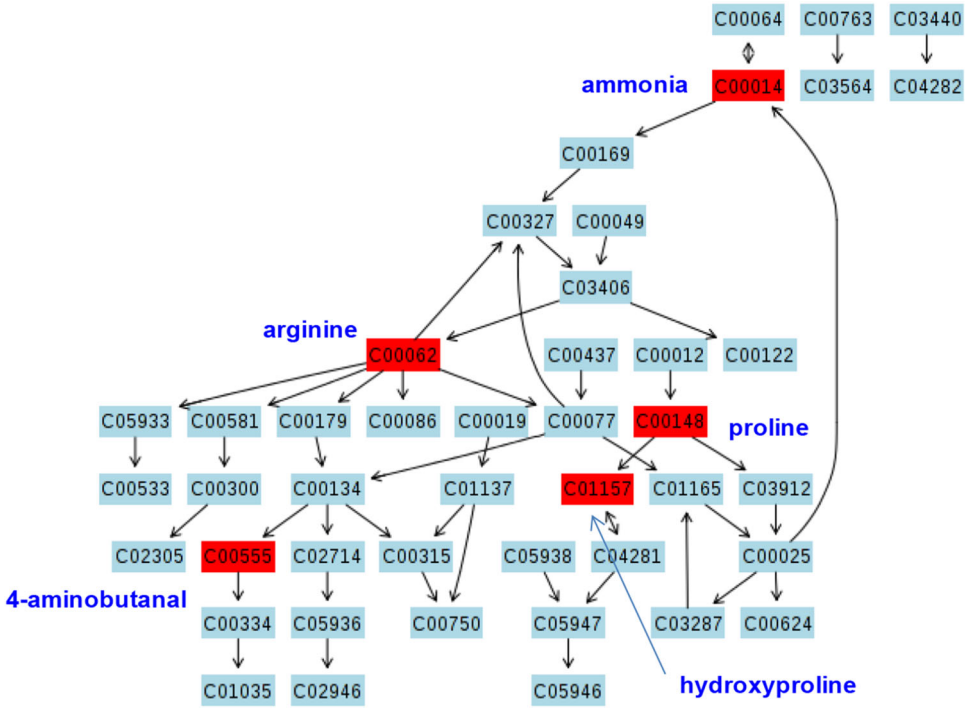

Fig. 5 Arginine-proline metabolic pathway with five metabolites, arginine, proline, ammonia, hydroxyproline, and 4-aminobutanal, found to be dysregulated by metabolomic analysis (*highlighted in red*) in the rat model of asthma (KEGG entry number is given for each metabolite) (Color figure online)

Table 2 Pearson correlation coefficients comparing metabolite levels and leucocyte numbers in bronchoalveolar lavage fluids

Metabolite	Total cell number	Eosinophils	Neutrophils	Macrophages
Formamide	0.88	NS	0.911	0.479
Proline	0.85	0.334	0.883	0.424
Ammonia	0.799	0.626	0.79	NS
Threonine	0.793	NS	0.84	NS
4-Aminobutanal	0.751	0.482	0.73	0.398
Valine	0.719	0.448	0.64	0.535
Alanine	0.711	0.446	0.716	NS
2-Phenylglycine	0.676	0.528	0.583	0.484
Arginine	0.641	0.485	0.6	0.343
Hydroxyproline	0.638	0.57	0.607	NS
Asparagine	0.637	0.44	0.613	NS
4-Hydroxybenzaldehyde	0.608	0.366	0.546	0.446
Xanthine	−0.423	−0.343	−0.386	NS

Moderate correlations are values of −0.5 to −0.3 (negative correlations) or 0.3–0.5; strong correlations are values of −1.0 to −0.5 (negative correlations) or strong correlations 0.5–1

NS no significant correlation

inflammation groups are statistically different than the numbers in the control group ($P < 0.001$). For the total leucocyte numbers (a) and the neutrophils (b) the differences between the low and high inflammation groups are statistically significant ($P < 0.001$), whereas for eosinophils and macrophages, there is no significant difference. Thus the overall metabolomic profile of BALF (Figs. 3a, 4) in this rat model of allergic inflammation is associated with the influx of neutrophils rather than eosinophils or macrophages. Pearson correlation analysis was used to identify if there is correlation between individual metabolites and the numbers of infiltrating leucocytes. Table 2 shows that among the 13 most significant metabolites there are 12 metabolites (excluding xanthine with a moderate negative correlation) with a strong positive correlation to neutrophils numbers (correlation coefficients from 0.546 to 0.911). There is very weak correlation between individual metabolites and macrophage numbers. Supplemental Table T6 shows the correlation coefficients of levels of individual metabolites compared to the percentages of leucocytes. Twelve of the metabolites have a strong positive correlation (one a negative correlation) with the percentage of neutrophils. There are 8 metabolites with a moderate positive correlation with the percentage of eosinophils and 13 metabolites with a strong negative correlation with the percentage of macrophages.

3.6 Discussion

Our first objective was to develop a metabolomic profiling method for rat BALF samples using dansylation isotopic labeling LC–MS that would allow the detection of many amine- and phenol-containing metabolites. Metabolites in this sub-metabolome are key components of several metabolic pathways. The dansyl labeling LC–MS method has been successfully applied for comprehensive metabolomic profiling of urine, cerebral spinal fluid, saliva, and cell extracts (Guo and Li 2009; Guo et al. 2011; Zheng et al. 2012; Wu and Li 2013; Wu et al. 2013). However, the typical dansyl labeling LC–MS protocol encountered difficulties with rat BALF samples containing phosphate saline buffer that caused ion suppression and metabolite dilution. Accordingly, we used SPE for sample cleanup and analyte enrichment prior to injection of the labeled samples into LC–MS.

There are several advantages of this workflow. Firstly, SPE after dansylation labeling can minimize sample loss, as the labeled metabolites have a higher hydrophobicity than their unlabeled counterparts and are more readily retained on the reversed phase SPE cartridge. Secondly, quantification accuracy and precision are improved by spiking ^{13}C-dansyl standards or internal control (i.e., pooled sample) into the ^{12}C-dansyl labeled sample before running SPE and concentrating the eluate. Thirdly, dansyl labeling improves sensitivity, allowing the detection of metabolites in nM concentrations, thus increasing the metabolome coverage. A previous NMR study of rat BALF showed small numbers of peaks detected in the NMR spectra with about 20 metabolites identified. In a recent study of BALF from mice 300 peaks were detected by LC–MS using both positive and negative ion modes. It has been estimated that >80 % of the peaks detected in LC–MS analysis of biofluids such as serum and urine are not related to the signals of metabolites and <20 % of those peaks could be assigned to unique metabolites (Jankevics et al. 2012). Thus, conventional LC–MS is not sufficiently sensitive to detect many metabolites in BALF. We detected 250 peak pairs or putative metabolites in rat BALF and identified 36 metabolites using authentic standards. We determined that the absolute concentrations of 15 metabolites ranged from 6.7 nM to 3.93 μM; another 9 metabolites were below the limit of quantification using the QTrap instrument (50 nM except 5 nM for cresol).

In addition to improved detectability, differential isotope labeling allows quantitative metabolomic profiling to reveal metabolic changes with high accuracy and precision. We used a pooled BALF sample labeled with ^{13}C-dansyl chloride as a control to compare the metabolite concentration changes among all the individual samples that were labeled separately with ^{12}C-dansyl chloride. The peak intensity ratio of the ^{12}C-/^{13}C-peak pair from a metabolite reflects the concentration of the metabolite in a sample relative to the control or pooled sample. As the same

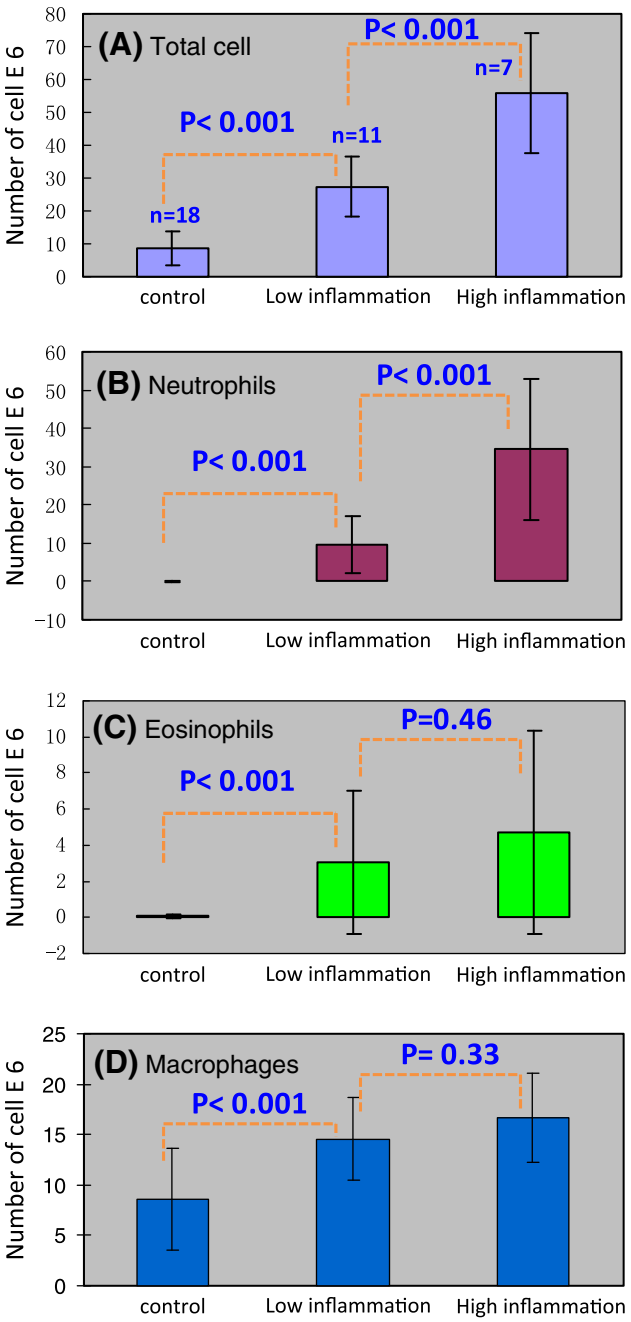

Fig. 6 Cell numbers (mean ± SD) in bronchoalveolar lavage fluids from control rats (n = 18, naive [n = 9] pooled with sensitized but saline challenged, n = 9) and sensitized rats challenged with aerosolized ovalbumin (n = 18). The sensitized, ovalbumin challenged rats are separated into two subgroups, low and high inflammation, based on metabolomic profiles (see text). **a** Total leucocyte numbers, **b** neutrophils, **c** eosinophils, and **d** macrophages; the *P* values between "low inflammation" and "high inflammation" subgroups are indicated, and also *P* values between control groups and "low inflammation" or "high inflammation" subgroups are indicated

control or pooled sample was used, the peak intensity ratios of a given peak pair determined in different samples could be used to gauge the relative concentration differences among these samples. These ratios from individual samples were analyzed by PCA and other statistics or chemometrics tools to determine the metabolomic variations between 18 control rats and 18 rats with airways inflammation.

Urine samples from human adults with asthma (Saude et al. 2011), children with asthma (Mattarucchi et al. 2012), and a guinea pig model of asthma (Saude et al. 2009) have been used to conduct metabolomic profiling and search for metabolite biomarkers of asthma. Urine metabolomics showed great potential for developing a noninvasive tool for diagnosis of asthma. However, urine might not directly reflect the pathophysiological status of lung tissue, the location of allergic inflammation. By contrast, BALF is a washing from the lumen of the lung, and studying the BALF metabolome is likely to better reflect the metabolomic changes associated with the pathophysiology of asthma. Indeed, using BALF from a strongly eosinophilic model of experimental asthma in the mouse, Ho et al. identified alterations in energy, amino acid and lipid metabolism in the lung (Ho et al. 2013). Previous urine studies identified some potential biomarkers associated with asthma, however, they did not report any dysregulated metabolic pathways. We established that the arginine-proline metabolic pathway was likely dysregulated in our rat model of allergic airways inflammation. None of those metabolites in arginine-proline pathway were reported in previous urine studies, and the mouse BALF study reported only 2-oxoargine, one of metabolites in arginine-proline pathway was affected by dexamethasone treatment used in human asthma. Our method has limitations as it targets metabolites containing primary, secondary, or phenol groups, but does not detect metabolites such as carbohydrate, lipid, sterol or organic acids, which were detected by GC–MS (Ho et al. 2013). Our lab is currently developing other isotope labeling LC methods to target those metabolites.

Various rat and mouse models of experimental asthma differ in the immunization protocols for OA, and often, perhaps most importantly, in the challenge protocols with aerosolized OA (e.g., d 21, 5 min, 5 % exposure in the rat; d 22, 23 and 24, 30 min, 1 % exposures in the mouse (Cheng et al. 2011). In our studies of sensitized rats following OA challenge, there is prominent neutrophilia in BALF (~19 %), as well as a modest eosinophilia (~3.7 %) and an increased number of macrophages as identified by several other workers (Elwood et al. 1991; Haczku et al. 1994; Schuster et al. 2000), whereas in the mouse model there is a prominent eosinophilia (>50 %) and only a modest neutrophilia (<5 %) (Ho et al. 2013). These distinct inflammatory cell infiltrates in the two models, as well as the number and duration of OA challenges, likely contribute to differences in lung metabolism seen. The pronounced neutrophilia in the rat is strongly associated with the metabolomic profile and several individual metabolites, whereas the lower eosinophilia is not associated with the overall metabolomic profile, but is moderately associated with 8 of 13 individual metabolites.

Arginine is an important metabolite of the urea cycle that can be metabolized into urea and ornithine by the enzyme arginase (King et al. 2004). Ornithine can serve as a substrate for ornithine decarboxylase, leading to downstream proline. Hydroxyproline is a product of proline hydrolyzed by 4-hydroxylase. Both proline and hydroxyproline are required for collagen synthesis, which is associated with pulmonary fibrosis (Ou et al. 2008; Zeki et al. 2010). Ornithine can also be a substrate for ornithine aminotransferase, which synthesizes polyamines such as putrescine. 4-Aminobutanal is a metabolite of putrescine using diamine oxidase. Polyamines and their metabolites may be involved in promotion of cell proliferation and differentiation (Benson et al. 2011). Therefore, our metabolomics data suggest that the arginine-proline metabolic pathway might play an important role in the pathogenesis of allergic asthma. Indeed, there is considerable evidence that dysregulated arginase and altered arginine metabolism are associated with asthma (Zimmermann et al. 2003; Lara et al. 2008). One of the earliest studies using global microarray analysis found that arginase isoforms I and II were dysregulated in lung samples from a mouse model of asthma (Zimmermann et al. 2003; King et al. 2004). Arginase expression was induced in the mouse model, as well as in humans with asthma. Arginase is mainly responsible for regulating arginine metabolism into urea and ornithine as well as downstream metabolites, such as putrescine, proline and hyroxyproline. Therefore our untargeted metabolomics data helps validate previous studies suggesting the importance of the arginine-proline metabolic pathway in the pathogenesis of asthma. Further studies are warranted to investigate the role of enzymes other than arginase in this metabolic pathway.

We identified that xanthine, an intermediate in the degradation of adenosine monophosphate to uric acid, was downregulated in allergic asthma. Although it is unclear whether it is associated with pathogenesis of asthma, it has been reported that xanthine could be used as a bronchodilator to treat asthma (Seddon et al. 2006).

Our metabolomic profiling of the rat model of allergic inflammation is associated with the influx of inflammatory cells into the airways, especially neutrophils and to a lesser extent eosinophils. Although eosinophilic airway inflammation is one pathological hallmark in allergic inflammation (Kamath et al. 2005), it does not explain the diversity of phenotypes of asthma in humans, and increased numbers

of neutrophils are associated with some severe asthma (Wenzel 2012). Given that proline and hydroxyproline dysregulation is associated with collagen deposition, the perturbed arginine-proline metabolic pathway we identified may be associated with neutrophil activation and function. However, several other cell types can be associated with collagen metabolism and the arginine-proline pathway and further study is needed to elucidate the relationship between the metabolomic profile of BALF and inflammatory cell numbers and their activities.

4 Concluding remarks

We have developed a new LC–MS method for analyzing the metabolome of rat BALF with much improved sensitivity. This method is based on differential $^{12}C/^{13}C$ dansyl labeling of BALF metabolites, SPE for analyte concentration, and LC–FTICR-MS for analysis. Dansylation selectively labels the amine- and phenol-containing metabolites and improves their separation in RPLC and detection in ESI–MS. We detected 250 peak pairs or putative metabolites in rat BALF, among which we could identify 36 metabolites. We applied this method to analyze the BALF metabolome of an experimental model of asthma. Comparative metabolomics using chemometrics methods including PCA, OPLS-DA and hierarchical clustering identified distinct separation between 18 control rats and 18 inflamed rats. Metabolic pathway analysis showed that the arginine-proline metabolic pathway was dysregulated in the rat model of allergic inflammation. Thus isotope labeling LC–MS can be used to improve metabolomic profiling of BALF. Future work in applying and developing other labeling chemistries targeting other functional groups will increase the overall metabolome coverage. Metabolomic profiling of BALF is a promising approach to studying asthma and has potential as a novel diagnostic tool in clinical settings. With improved coverage, metabolome profiles of BALF may also help monitor the effect of various therapeutics on asthma (Saude et al. 2011; Ho et al. 2013).

Acknowledgments This work was funded by the Natural Sciences and Engineering Research Council of Canada, the Canada Research Chairs program, Genome Canada, Genome Alberta, the Canadian Institutes for Health Research and AllerGen NCE Inc.

References

Adamko, D. J., Sykes, B. D., & Rowe, B. H. (2012). The metabolomics of asthma: Novel diagnostic potential. *Chest, 141*(5), 1295–1302.

Atzei, A., Atzori, L., Moretti, C., Barberini, L., Noto, A., Ottonello, G., et al. (2011). Metabolomics in paediatric respiratory diseases and bronchiolitis. *Journal of Maternal-Fetal & Neonatal Medicine, 24*, 60–63.

Azmi, J., Connelly, J., Holmes, E., Nicholson, J. K., Shore, R. F., & Griffin, J. L. (2005). Characterization of the biochemical effects of 1-nitronaphthalene in rats using global metabolic profiling by NMR spectroscopy and pattern recognition. *Biomarkers, 10*(6), 401–416.

Benson, R. C., Hardy, K. A., & Morris, C. R. (2011). Arginase and arginine dysregulation in asthma. *Journal of Allergy, 2011*(2011), 736319.

Carraro, S., Rezzi, S., Reniero, F., Heberger, K., Giordano, G., Zanconato, S., et al. (2007). Metabolomics applied to exhaled breath condensate in childhood asthma. *American Journal of Respiratory and Critical Care Medicine, 175*(10), 986–990.

Cheng, C., Ho, W. E., Goh, F. Y., Guan, S. P., Kong, L. R., Lai, W. Q., et al. (2011). Anti-malarial drug artesunate attenuates experimental allergic asthma via inhibition of the phosphoinositide 3-kinase/Akt pathway. *PLoS ONE, 6*(6), 9.

Connett, G. J. (2000). Bronchoalveolar lavage. *Paediatric Respiratory Reviews, 1*(1), 52–56.

Dery, R. E., Ulanova, M., Puttagunta, L., Stenton, G. R., James, D., Merani, S., et al. (2004). Inhibition of allergen-induced pulmonary inflammation by the tripeptide feG: A mimetic of a neuro-endocrine pathway. *European Journal of Immunology, 34*(12), 3315–3325.

Elwood, W., Lotvall, J. O., Barnes, P. J., & Chung, K. F. (1991). Characterization of allergen-induced bronchial hyperresponsiveness and airway inflammation in actively sensitized brown-Norway rats. *Journal of Allergy and Clinical Immunology, 88*(6), 951–960.

Fabiano, A., Gazzolo, D., Zimmermann, L. J. I., Gavilanes, A. W. D., Paolillo, P., Fanos, V., et al. (2012). Metabolomic analysis of bronchoalveolar lavage fluid in preterm infants complicated by respiratory distress syndrome: Preliminary results. *Journal of Maternal-Fetal & Neonatal Medicine, 24*(S2), 56–59.

Galli, S. J., Tsai, M., & Piliponsky, A. M. (2008). The development of allergic inflammation. *Nature, 454*(7203), 445–454.

Guo, K., Bamforth, F., & Li, L. A. (2011). Qualitative metabolome analysis of human cerebrospinal fluid by 13C-/12C-isotope dansylation labeling combined with liquid chromatography Fourier transform ion cyclotron resonance mass spectrometry. *Journal of the American Society for Mass Spectrometry, 22*(2), 339–347.

Guo, K., & Li, L. (2009). Differential 12C-/13C-isotope dansylation labeling and fast liquid chromatography/mass spectrometry for absolute and relative quantification of the metabolome. *Analytical Chemistry, 81*(10), 3919–3932.

Haczku, A., Moqbel, R., Elwood, W., Sun, J., Kay, A. B., Barnes, P. J., et al. (1994). Effects of prolonged repeated exposure to ovalbumin in sensitized brown Norway rats. *American Journal of Respiratory and Critical Care Medicine, 150*(1), 23–27.

Ho, W. E., Xu, Y. J., Xu, F. G., Cheng, C., Peh, H. Y., Tannenbaum, S. R., et al. (2013). Metabolomics reveals altered metabolic pathways in experimental asthma. *American Journal of Respiratory Cell and Molecular Biology, 48*(2), 204–211.

Hu, J. Z., Rommereim, D. N., Minard, K. R., Woodstock, A., Harrer, B. J., Wind, R. A., et al. (2008). Metabolomics in lung inflammation: A high-resolution H-1 NMR study of mice exposed to silica dust. *Toxicology Mechanisms and Methods, 18*(5), 385–398.

Jankevics, A., Merlo, M. E., de Vries, M., Vonk, R. J., Takano, E., & Breitling, R. (2012). Separating the wheat from the chaff: A prioritisation pipeline for the analysis of metabolomics datasets. *Metabolomics, 8*(1), S29–S36.

Kamath, A. V., Pavord, I. D., Ruparelia, P. R., & Chilvers, E. R. (2005). Is the neutrophil the key effector cell in severe asthma? *Thorax, 60*(7), 529–530.

King, N. E., Rothenberg, M. E., & Zimmermann, N. (2004). Arginine in asthma and lung inflammation. *Journal of Nutrition, 134*(10), 2830S–2836S.

Kominsky, D. J., Campbell, E. L., & Colgan, S. P. (2010). Metabolic shifts in immunity and inflammation. *Journal of Immunology, 184*(8), 4062–4068.

Lara, A., Khatri, S. B., Wang, Z., Comhair, S. A. A., Xu, W., Dweik, R. A., et al. (2008). Alterations of the arginine metabolome in asthma. *American Journal of Respiratory and Critical Care Medicine, 178*(7), 673–681.

Li, L., Li, R. H., Zhou, J. J., Zuniga, A., Stanislaus, A. E., Wu, Y. M., et al. (2013). MyCompoundID: Using an evidence-based metabolome library for metabolite identification. *Analytical Chemistry, 85*(6), 3401–3408.

Locksley, R. M. (2010). Asthma and allergic inflammation. *Cell, 140*(6), 777–783.

Maghni, K., Taha, R., Afif, W., Hamid, Q., & Martin, J. G. (2000). Dichotomy between neurokinin receptor actions in modulating allergic airway responses in an animal model of helper T cell type 2 cytokine-associated inflammation. *American Journal of Respiratory and Critical Care Medicine, 162*(3), 1068–1074.

Mattarucchi, E., Baraldi, E., & Guillou, C. (2012). Metabolomics applied to urine samples in childhood asthma; differentiation between asthma phenotypes and identification of relevant metabolites. *Biomedical Chromatography, 26*(1), 89–94.

Meyer, K. C. (2004). The role of bronchoalveolar lavage in interstitial lung disease. *Clinics in Chest Medicine, 25*(4), 637–640.

Ou, X. M., Feng, Y. L., Wen, F. Q., Huang, X. Y., Xiao, J., Wang, K., et al. (2008). Simvastatin attenuates bleomycin-induced pulmonary fibrosis in mice. *Chinese Medical Journal, 121*(18), 1821–1829.

Reynolds, H. Y. (2000). Use of bronchoalveolar lavage in humans—Past necessity and future imperative. *Lung, 178*(5), 271–293.

Saude, E. J., Obiefuna, I. P., Somorjai, R. L., Ajamian, F., Skappak, C., Ahmad, T., et al. (2009). Metabolomic biomarkers in a model of asthma exacerbation urine nuclear magnetic resonance. *American Journal of Respiratory and Critical Care Medicine, 179*(1), 25–34.

Saude, E. J., Skappak, C. D., Regush, S., Cook, K., Ben-Zvi, A., Becker, A., et al. (2011). Metabolomic profiling of asthma: Diagnostic utility of urine nuclear magnetic resonance spectroscopy. *Journal of Allergy and Clinical Immunology, 127*(3), 757–764.

Schuster, M., Tschernig, T., Krug, N., & Pabst, R. (2000). Lymphocytes migrate from the blood into the bronchoalveolar lavage and lung parenchyma in the asthma model of the brown Norway rat. *American Journal of Respiratory and Critical Care Medicine, 161*(2), 558–566.

Seddon, P., Bara, A., Ducharme, F. M., & Lasserson, T. J. (2006). Oral xanthines as maintenance treatment for asthma in children. Cochrane Database of Systematic Reviews (1), 131.

Serkova, N. J., Van Rheen, Z., Tobias, M., Pitzer, J. E., Wilkinson, J. E., & Stringer, K. A. (2008). Utility of magnetic resonance imaging and nuclear magnetic resonance-based metabolomics for quantification of inflammatory lung injury. *American Journal of Physiology-Lung Cellular and Molecular Physiology, 295*(1), L152–L161.

Smith, C. A., Want, E. J., O'Maille, G., Abagyan, R., & Siuzdak, G. (2006). XCMS: Processing mass spectrometry data for metabolite profiling using nonlinear peak alignment, matching, and identification. *Analytical Chemistry, 78*(3), 779–787.

Szefler, S. J., Wenzel, S., Brown, R., Erzurum, S. C., Fahy, J. V., Hamilton, R. G., et al. (2012). Asthma outcomes: Biomarkers. *Journal of Allergy and Clinical Immunology, 129*(3), S9–S23.

Walters, E., Ward, C., & Li, X. (1996). Bronchoalveolar lavage in asthma research. *Respirology, 1*(4), 233–245.

Waserman, S., Olivenstein, R., Renzi, P., Xu, L. J., & Martin, J. G. (1992). The relationship between late asthmatic responses and antigen-specific immunoglobulin. *Journal of Allergy and Clinical Immunology, 90*(4), 661–669.

Wenzel, S. E. (2012). Asthma phenotypes: The evolution from clinical to molecular approaches. *Nature Medicine, 18*(5), 716–725.

Wishart, D. S., Knox, C., Guo, A. C., Eisner, R., Young, N., Gautam, B., et al. (2009). HMDB: A knowledgebase for the human metabolome. *Nucleic Acids Research, 37*, D603–D610.

Wolak, J. E., Esther, C. R., & O'Connell, T. M. (2009). Metabolomic analysis of bronchoalveolar lavage fluid from cystic fibrosis patients. *Biomarkers, 14*(1), 55–60.

Wu, Y. M., & Li, L. (2013). Development of isotope labeling liquid chromatography-mass spectrometry for metabolic profiling of bacterial cells and its application for bacterial differentiation. *Analytical Chemistry, 85*(12), 5755–5763.

Wu, M., Yates, S., Zurek, G., & Barsch, A. (2013). Metabolomics studies on yeast arginine synthesis pathway mutants using maXis impact with ionBooster, Application Note #ET-33: 2013. Bruker Daltonik GmbH, Breman, Germany.

Xia, J. G., Psychogios, N., Young, N., & Wishart, D. S. (2009). MetaboAnalyst: A web server for metabolomic data analysis and interpretation. *Nucleic Acids Research, 37*, W652–W660.

Xia, J. G., & Wishart, D. S. (2010). MetPA: A web-based metabolomics tool for pathway analysis and visualization. *Bioinformatics, 26*(18), 2342–2344.

Zeki, A. A., Bratt, J. M., Rabowsky, M., Last, J. A., & Kenyon, N. J. (2010). Simvastatin inhibits goblet cell hyperplasia and lung arginase in a mouse model of allergic asthma: A novel treatment for airway remodeling? *Translational Research, 156*(6), 335–349.

Zheng, J. M., Dixon, R. A., & Li, L. (2012). Development of isotope labeling LC–MS for human salivary metabolomics and application to profiling metabolome changes associated with mild cognitive impairment. *Analytical Chemistry, 84*(24), 10802–10811.

Zimmermann, N., King, N. E., Laporte, J., Yang, M., Mishra, A., Pope, S. M., et al. (2003). Dissection of experimental asthma with DNA microarray analysis identifies arginase in asthma pathogenesis. *Journal of Clinical Investigation, 111*(12), 1863–1874.